Emergent Materials (2019) 2:327–335
https://doi.org/10.1007/s42247-019-00041-9

ORIGINAL ARTICLE

# Eco-friendly synthesis and characterization of phytogenic zero-valent iron nanoparticles for efficient removal of Cr(VI) from contaminated water

Kallepally Sravanthi[1] · Dasari Ayodhya[1] · Parikibandla Yadagiri Swamy[1]

Received: 27 September 2018 / Accepted: 10 July 2019 / Published online: 25 July 2019


## Abstract

Zero-valent iron nanoparticles (ZVIN) are widely synthesized by several methods in the last decades because it offers indisputable advantages to almost every area of expertise, heavy metal ions removal, environmental remediation including for the wastewater treatment. Herein, we report for the first time, the green and eco-friendly synthesis of phytogenic ZVIN using reproducible *Catharanthus roseus* (CR) flower extract for the removal of heavy metal ions including Cr(VI) by adsorption isotherms. The synthesized stable ZVIN were characterized by UV-visible absorption spectroscopy (UV-vis), Fourier-transform infrared (FT-IR), X-ray diffraction (XRD), scanning electron microscopy (SEM), and energy-dispersive X-ray spectroscopy (EDX). The FT-IR analysis reveals that the polyphenolic compounds that are present in the CR flower extract may be responsible for the reduction and stabilization of the ZVIN. The XRD and SEM-EDX analyses confirmed the phase, composition of elements and morphology of the ZVIN. The synthesized low-cost and non-toxic ZVIN used for the adsorption removal of Cr(VI) from contaminated water; and the Langmuir and Freundlich adsorption isotherms are used to study the adsorption process by the experimental equilibrium adsorption data. The maximum removal of Cr(VI) (98.28%) was observed using optimal conditions of 1.6 g/L of ZVIN concentration, 10 ppm of Cr(VI) concentration, and pH = 4.3 of the initial solution. The adsorption removal of Cr(VI) using the synthesized ZVIN as follows pseudo-second-order kinetic equation with a corresponding correlation coefficient of ($R^2 = 0.99$).

**Keywords** ZVIN · *Catharanthus roseus* flower extract · Cr(VI) removal · Adsorption isotherms · Kinetics

## 1 Introduction

Contamination of air, water, and soil by toxic heavy metal ions is one of the serious environmental problems faced by the world today. Heavy metals represent a group of dangerous environmental pollutants and due to toxic effects on human health in concentrations above the permissible limits, cause widespread concerns [1]. Non-degradable heavy metals also can accumulate in living tissues and enter into the food chain which causes huge damage to the biosphere in the form of various diseases and disorders [1–5]. Among all, hexavalent chromium (Cr(VI)) is one of the most hazardous heavy metal ions in nature. With the industrialization, a large quantity of wastewater containing high concentrations of Cr(VI) is released into the environment from distinct industrial activities, including iron and steel manufacturing, electroplating, metal cleaning, preservation of food, leather tanning, pigment production, and other anthropogenic sources [2–5]. The Cr(VI) metal ion is highly toxic to human and animal tissues because of its potential carcinogenic, teratogenic, and mutagenic properties [5–8]. In general, Cr(VI) may be in the form of negatively charged oxyanions such as dichromate ($Cr_2O_7^{-2}$) or chromate ($CrO_4^{-2}$) or hydrogen chromate ($HCrO_4^-$) in solutions. As highly soluble Cr(VI) is freely transferred in aqueous environments due to repulsive electrostatic interactions among anionic Cr(VI) species and negatively charged particles of soil, it is necessary to remove Cr(VI)

✉ Dasari Ayodhya
ayodhyadasari@gmail.com

✉ Parikibandla Yadagiri Swamy
parikibandla@gmail.com

Kallepally Sravanthi
kallepally.sravanthi@gmail.com

[1] Department of Chemistry, Osmania University, Hyderabad, Telangana 500007, India

from industrial wastewater before entering into the environment.

Several methods are investigated for the removal of heavy metals such as filtration, ion exchange, precipitation, membrane process, sedimentation, electrochemical treatment, reverse osmosis, photocatalytic reduction, and adsorption [9–12]. Out of these, adsorption is considered more preferable for eliminating heavy metals due to its unique properties like ease of operation, the simplicity of design, insensitivity to toxic pollutants, fewer amounts of harmful substances, and low cost [13, 14]. There are many eco-friendly bioadsorbents, but those show poor adsorption capacity and very slow process kinetics. But nowadays, nanoscale zero-valent iron is widely used for the adsorptive removal of heavy metals due to its large specific surface area, high reactivity of surface sites, small particle size, and strong reducibility [15, 16].

Mostly, ZVIN are synthesized by a liquid-phase reduction method using sodium borohydride or potassium borohydride as reducing agents [17]. But the main disadvantage of this method is toxicity of borohydride which eventually may induce environmental pollution in the form of resulting ZVIN. Furthermore, ZVIN prepared by this method can agglomerate quickly in clusters. Hence, to prevent agglomeration process, it is required to add some dispersant agents like stabilizing or capping agents [18, 19]. If non-biodegradable dispersant agents used in large scale, then those are treated as secondary pollutants. Therefore, there is a clear need for novel alternative method which obeys the tenets of green chemistry, for the preparation of ZVIN. In the process of green chemistry, the plant extract mediated synthesis which is economically preferable and environmentally compatible has been proposed as a preparative method for ZVIN [20, 21]. Naturally, plant extracts contain polyphenols, flavonoids, and other phytochemicals that can act as both reducing and stabilizing agents [22, 23]. Thus, the biomolecules that are present in plant extracts can reduce ferrous or ferric ions to zero-valent iron and effectively prevent agglomeration of ZVIN [23, 24].

From the inspiration of several, methods were utilized for the synthesis of ZVIN using green techniques for avoiding toxic and high-expensive materials for the prevention of environmental pollution. In this study, green, eco-friendly and low-cost synthesis of CR flower extract mediated and stabilized ZVIN was first time reported for the effective adsorptive removal of Cr(VI) from the contaminated water. The optimization factors for Cr(VI) removal from aqueous solution using CR flower extract stabilized ZVIN under different variables namely, pH of the aqueous solution, the concentration of ZVIN (g/L), the dosage of ZVIN, contact time, and initial concentration of Cr(VI) were also investigated.

## 2 Experimental

### 2.1 Materials

Ferric nitrate nonahydrate ($FeNO_3 \cdot 9H_2O$, CAS Number 7782-61-8), potassium dichromate ($K_2Cr_2O_7$, CAS Number 7778-50-9), lead nitrate ($Pb(NO_3)_2$, CAS Number 10099-74-8), and ethyl alcohol ($CH_3CH_2OH$, CAS Number 64-17-5) were purchased AR grade from Sigma Aldrich Chemicals, India. The fresh flowers of *Catharanthus roseus* were collected from Osmania University, Hyderabad, India.

### 2.2 Collection of Catharanthus roseus flower extract

*Catharanthus roseus* flowers are washed twice with double distilled water and then cut into small pieces and dried. The CR flower extract was prepared by mixing 20 mg weight of dried flower extract powder with 100 mL double distilled water in a 250-mL conical flask and boiled for 5 min at 100 °C. After cooling, the solution is filtered by Whatman's no.1 filter paper and the filtration carried out thrice to get a clear extract solution.

### 2.3 Eco-friendly preparation of ZVIN

The green and eco-friendly stable ZVIN are prepared by CR flower extract as a reducing and stabilizing agent. In this typical synthesis, 0.01 M $FeNO_3 \times 9H_2O$ (ferric nitrate nonahydrate) is prepared in double distilled water and mixed with flower extract in 1:1 volume ratio. For the reduction of $Fe^{+3}$ ions as $Fe^0$ to take place, the equal volume of CR flower extract is added slowly to aqueous ferric nitrate solution with constant stirring for 15 min by using magnetic stirrer and the reaction is carried out at room temperature. During the synthesis process, the formation of ZVIN indicated by the change of color of the reaction mixture to black color due to the phenolic content (polyphenols) of CR flower extract interacted with the ferric ions [25]. Afterward, the reaction mixture is centrifuged at 15,000 rpm for 15–20 min and next to the collected precipitate is washed with 1:1 ethanol water and double distilled water several times to remove remaining impurities. Finally, the obtained black ZVIN precipitate is dried at 60 °C in an oven for 24 h and stored for further applications. The synthesis procedure of CR flower extract stabilized ZVIN was explained graphically and shown in Scheme 1.

### 2.4 Characterization techniques

UV-visible absorption analysis was carried out using UV-3600 spectrophotometer (Shimadzu) in the range of 200–800 nm. Scanning electron microscope (SEM) imaging analysis of the samples was conducted using a Zeiss evo18

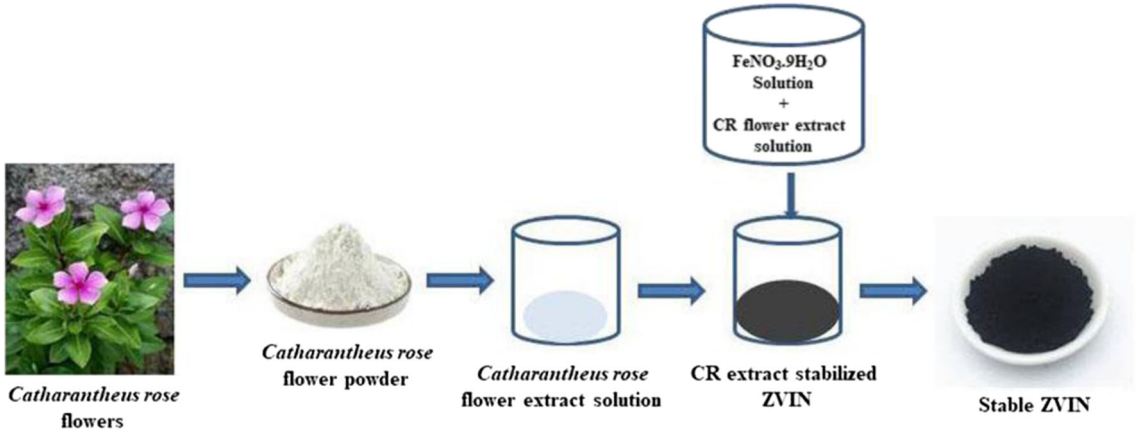


**Scheme 1** The schematic representation of the preparation of ZVIN using CR flower extract

scanning electron microscope with an equipment of EDX. The crystallinity and phase were examined using X-ray diffraction (XRD) analysis with a computer-controlled X-ray diffractometer (Philips, X'pert pro diffractometer) and equipped with a stepping motor and graphite crystal monochromator in the range $2\theta = 10–80°$. The FT-IR spectra of the synthesized ZVIN were analyzed by Bruker spectrophotometer in the range of wavenumber 400–4000 $cm^{-1}$.

## 2.5 Batch adsorption experiments for Cr(VI) removal

A series of batch adsorption experiments were tested to evaluate the efficiency of synthesized ZVIN for the removal of Cr(VI) from contaminated water with the variation of ZVIN concentration, Cr(VI) concentration, contact time, and pH of the initial solution by adsorption using UV-vis spectroscopy at room temperature. In this batch adsorption experiments, 30 mg of ZVIN mixed with 30 mL of potassium dichromate solution of different concentrations (10–100 ppm) and shaken uniformly for 2 h to carry out the adsorption studies. To examine the effect of contact time on the removal of Cr(VI), 100 mg of ZVIN is added to 250 mL of potassium dichromate (20 ppm) and stirred for a certain period of time on a magnetic stirrer. At certain time intervals (15, 30, 45, 60, and 120 min), about 5 mL of the aliquot was taken from the mixture and centrifuged to remove ZVIN. The experiments were conducted at the initial solution pH from 4.3 to 10.0 to examine the influence of CR flower extract stabilized ZVIN concentration and initial concentration of Cr(VI) on Cr(VI) removal efficiency. The concentration of Cr(VI) remaining in the solution is determined using spectrophotometer by measuring absorbance at $\lambda = 323$ nm. The reduction in the concentration of Cr(VI) is calculated from the difference between initial and final equilibrium concentrations. The removal efficiency is computed from the following equation:

$$\%of\ \text{Removal} = \frac{(c_0 - c_e)}{c_0} \times 100 \tag{1}$$

where $c_0$ and $c_e$ are total dissolved and equilibrium liquid-phase concentrations (mg $L^{-1}$), respectively.

## 2.6 Adsorption isotherms

Langmuir and Freundlich's models are applied to the equilibrium experimental data to predict the adsorption mechanism of Cr (VI) removal using CR flower extract stabilized ZVIN.

.

**Langmuir model** The important assumption of this model is the formation of a monolayer, i.e., the adsorbed layer contains the thickness of one molecular level [26]. Langmuir model is mainly applicable for a homogeneous surface. In this study, all active sites are identical, adsorption occurs at the definite number of localized sites, and hence adsorption energy is uniform. Even on adjacent active sites also, the intermolecular interactions and steric hindrances among adsorbed molecules are not noticeable. During the sorption process, each molecule has the same and constant enthalpies and activation energies. On the plane of adsorbent surface, no transmigration of adsorbed molecules takes place. The expression of Langmuir that relates molecules adsorbed on the solid surface to the equilibrium concentration of liquid phase molecules which are present above the surface of sorbent is given by the following equation:

$$q_e = \frac{X_m b c_e}{1 + b c_e} \tag{2}$$

where $q_e$ (mg $g^{-1}$) and $c_e$ (mg $L^{-1}$) are the amounts adsorbed on the surface of a unit mass of sorbent and the concentration of adsorbate in the solution at equilibrium, respectively. $X_m$ (mg $g^{-1}$) is the maximal adsorption capacity and $b$ (L $mg^{-1}$) gives affinity of binding sites (empirical constant). The Langmuir expression can be given in the linearized form:

$$\frac{c_e}{q_e} = \frac{1}{X_m} c_e + \frac{1}{X_m b} \quad (3)$$

**Freundlich model** It is a two-parameter earliest model and initially developed for animal charcoal adsorbent. The main assumption of the Freundlich model is adsorption occuring at the heterogeneous adsorbent surface with non-uniform distribution of enthalpies of adsorption [27]. The adsorption process is reversible, non-ideal multilayer formation takes place, and does not limit to monolayer sorption. The binding sites are not identical; every site is speculated to have different bond energies, the stronger site occupied first and the total amount of adsorbed adsorbate is considered to be a sum of adsorbate at all active sites. Hence, at the end of the adsorption process obviously adsorption energy decreases. The expression for Freundlich adsorption isotherm is as follows:

$$q_e = K_f c_e^{1/n} \quad (4)$$

where, $q_e$ (mg $g^{-1}$) and $c_e$ (mg $L^{-1}$) are the quantity adsorbed on the surface of a unit mass of sorbent and the concentration of adsorbate in the solution at equilibrium, respectively. $K_f$ (mg $g^{-1}$(L $mg^{-1}$)$^{1/n}$) is Freundlich constants which give the sorption capacity and $n$ indicates favorability of adsorption. Here '$n$' value gives information about the magnitude of driving force of adsorption and heterogeneity of binding sites. The values of $n$ between 1 and 10 ($1 < n < 10$) indicate favorable adsorption [28]. To calculate the values of Freundlich constants ($K_f$ and $n$) are summarized in Table 1, the equation of the linear form of Freundlich isotherm was taken as follows:

$$\log q_e = \log K_f + \frac{1}{n} \log c_e \quad (5)$$

## 3 Results and discussion

### 3.1 UV-vis absorption analysis

To determine the formation of ZVIN using UV-vis absorption spectra was carried out from 200 to 800 nm at room temperature (Fig. 1). The UV-vis spectral analysis of the clear solution of CR flower extract shows strong absorption in the region from 300 to 400 nm initially. It reveals the information about the presence of phytochemicals like polyphenols, amino acids, lipids, and carbohydrates [29]. After mixing the clear solution of CR flower extract to the ferric solution, the formation of a black color colloidal solution appears immediately. In the spectra of the colloidal solution, it was observed that strong absorption peaks of flower extract at 300 to 400 nm disappeared and a broad absorption peak appeared at higher wavelengths (Fig. 1). After that, the UV-vis absorption spectra of CR flower extract stabilized ZVIN does not exhibit any peaks indicating the dispersed pellets of ZVIN in aqueous solution. It revealed the formation of polydispersed ZVIN.

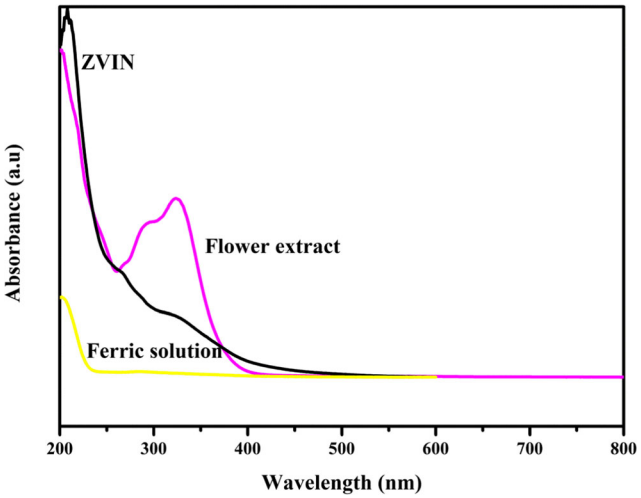


**Fig. 1** The UV-visible absorption spectra of flower extract, ferric solution, and ZVIN

**Table 1** The calculated Langmuir and Freundlich adsorption parameters for removal of Cr(VI) using ZVIN

| Langmuir model | | Freundlich model | |
|---|---|---|---|
| $X_m$ (mg $g^{-1}$) | 5.8 | $K_f$ (mg $g^{-1}$(L $mg^{-1}$)$^{1/n}$) | 2.88 |
| $B$ (L $mg^{-1}$) | 0.19 | $n$ | 6.6 |
| $R^2$ | 0.99 | $R^2$ | 0.96 |

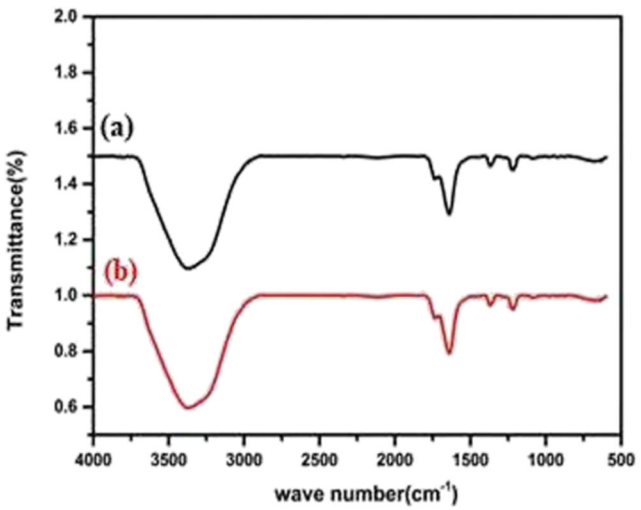


**Fig. 2** The FT-IR spectra of **a** CR flower extract stabilized ZVIN and **b** CR flower extract

### 3.2 FT-IR analysis

FT-IR spectra of CR flower extract and ZVIN stabilized in flower extract (Fig. 2) provide the information about formation and stabilization of iron nanoparticles by revealing the interaction among biomolecules of flower extract and metal ions. In the FT-IR spectral analysis of CR flower extract (Fig. 2a), it exhibited a strong absorption peak positioned at 3359 $cm^{-1}$ is due to -OH and -NH stretching vibrations and the peaks at 1641 $cm^{-1}$ and 1239 $cm^{-1}$ indicate the presence of amide group [30]. Furthermore, a peak positioned at 1083 $cm^{-1}$ gives the information about the presence of -OH bending and C-O-C stretching modes. These absorption peaks indicated the presence of polyphenols in CR flower extract [31, 32]. In the FT-IR spectrum of the colloidal solution of ZVIN stabilized in flower extract, it is observed that a peak positioned at 3359 is shifted to 3361 $cm^{-1}$ and peak at 1641 is shifted to 1645 $cm^{-1}$ with increasing intensity. Similarly, the peaks at 1239, 1083, 976 cm, and 923 shifted to 1231, 1078, 972, and 918 $cm^{-1,}$ respectively. The complete absence of peaks is also noticed at positions of 873 $cm^{-1}$ and 680 $cm^{-1}$ in ZVIN colloidal solution. The shifted peaks suggest that amide groups in CR flower extract may be involved in the formation of ZVIN and responsible for the reduction of $Fe^{+3}$ ions as $Fe^{0}$ [33, 34].

### 3.3 XRD analysis

The XRD analysis is carried out in the range of $2\theta$ value from 10 to 80° to investigate the crystalline structure and crystal size of synthesized CR flower extract stabilized ZVIN. In the XRD pattern of ZVIN prepared by CR flower extract (Fig. 3), the diffraction peaks at $2\theta$ of 44.5° (4 0 0) and 62.1° (4 4 0) indicate that the sample contains preponderantly zero-valent iron and the diffraction peak at $2\theta$ of 35.2° (3 1 1) is due to slight oxidation of iron [35]. In addition to the characteristic diffraction peaks of iron nanoparticles, very low-intensity peaks in between the $2\theta$ values of 20–25° are noticed due to the coating of organic matter on the surface of ZVIN, which serves to enhance particle stability. Using peak broadening profile of peak at the $2\theta$ value of 44.5°, the approximate size of ZVIN is calculated by Debye-Scherer's formula:

$$D = 0.94\,(\lambda)/\beta\cos\theta \tag{6}$$

where $\lambda$ is wavelength (1.5418 Å), $\theta$ is the diffraction angle, and $\beta$ is full-width at half maximum (FWHM) of corresponding peak. The calculated crystal size of synthesized ZVIN is approximately 20–30 nm from the Debye-Scherer's equation.

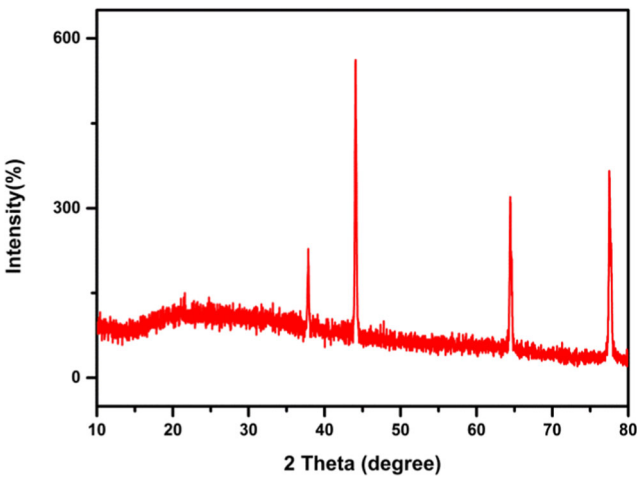


**Fig. 3** The powder XRD pattern of CR flower extract stabilized ZVIN

### 3.4 SEM and EDX analysis

To investigate the morphology, crystal growth, and approximate size of synthesized ZVIN by the SEM analysis and the corresponding SEM image is shown in Fig. 4a. It reveals that the ZVIN are not standalone, mostly spherical that they do not form a chain and some are irregular in shape. They are polydispersed with different sizes with less than 100 nm. In the SEM image of ZVIN, the slight agglomeration was observed due to the magnetic interactions among prepared

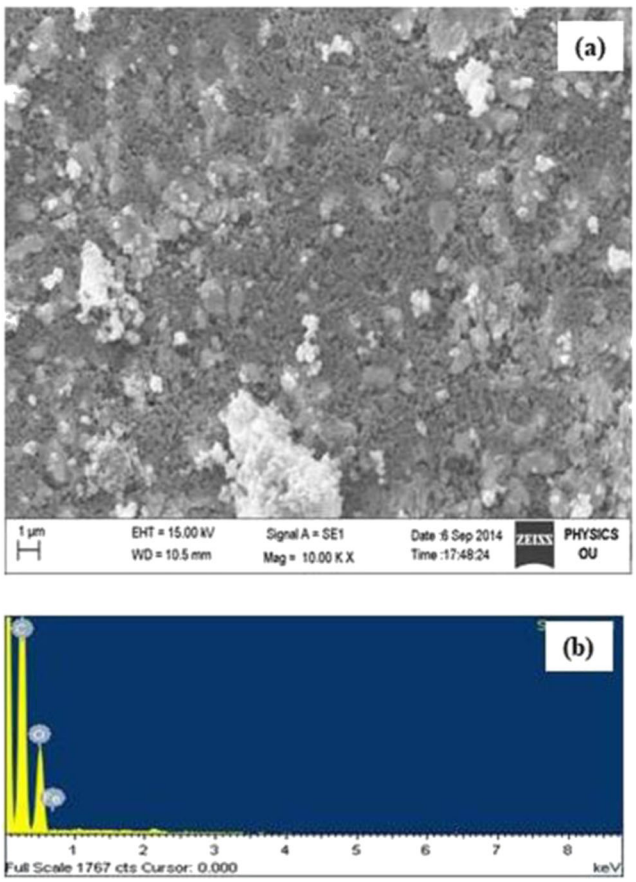


**Fig. 4** **a** SEM and **b** EDX images of CR flower extract stabilized ZVIN

nanoparticles and it shows some spherical shape of the small size particles is present. EDX analysis provides the qualitative as well as quantitative information about elements that may be involved in the formation of nanoparticles and is shown in Fig. 4b. It reveals the proportion of atomic percentages of iron (32.17%), carbon (44.24%), and oxygen (23.59%) elements present in the synthesized ZVIN. These results demonstrate that phytochemicals having the antioxidant property such as polyphenols, amino acids, reducing sugars, and nitrogenous bases present in the flower extract are responsible for the reduction of metal ions in the metal salt solution [36].

## 3.5 Effect of factors on Cr(VI) removal

Previous reports have been shown that many parameters influence the Cr(VI) removal ability of ZVIN in triplicate times for the optimization of parameters. In this study, the major factors known to Affect the reactivity, including the initial concentration of Cr(VI), contact time, pH, and ZVIN dosage are investigated for the removal of Cr(VI) from the contaminated water by adsorption technique.

### 3.5.1 Effect of initial concentration of Cr(VI)

From the experimental data, it is noticed that the initial concentration of Cr(VI) interacting with ZVIN increases and the removal efficiency decreases (Fig. 5). The percentage of removal of Cr(VI) in the solutions (10 ppm, 20 ppm, 40 ppm, 60 ppm, 80 ppm, and 100 ppm) in 2 h contact time are 99.5%, 99.1%, 80.2%, 74.6%, 66.4%, and 57.2%, respectively. The removal capacity of ZVIN is highest in Cr(VI) concentration at 10 ppm level. These experimental results are in good agreement with the previous report [37]. For a given amount of ZVIN, there exists a fixed number of binding sites to interact with Cr (VI) in solution and as the concentration of Cr(VI) increases, there is no corresponding increase in the binding sites as well as surface area of synthesized ZVIN. Therefore, in this investigation provided that at higher concentrations of Cr (VI), the removal efficiency of ZVIN is less.

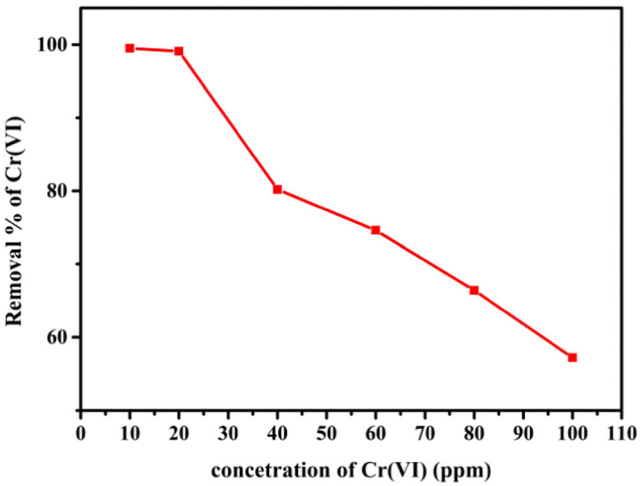


**Fig. 5** Effect of the initial concentration of Cr(VI) on % of removal using ZVIN

### 3.5.2 Effect of contact time

Initially, the removal rate of Cr(VI) in contaminated water is more but as the time increases, the rate of removal decreases and stable after reaching the equilibrium state which agrees with experimental results of the effect of initial concentration of Cr (VI) and it was shown in Fig. 6a, b. These results clearly revealed the dependence of the rate of removal on the initial concentration of Cr(VI).

### 3.5.3 Effect of solution pH on Cr(VI) removal

The pH of the solution shows a vital role in the adsorptive removal process of heavy metals due to the surface charge and distribution of binding sites of adsorbent are greatly influenced by the pH of the solution. Therefore, adsorption ability of adsorbent and charge of the metal ion in the solution both are controlled in response to pH of the medium. In this study, the original pH of the Cr(VI) solution without adjustment is 4.3 and the influence of pH on the removal of Cr(VI) is investigated by considering the pH range from 4.3 to10.0. When the pH is less than 4.3, it was not taken into account due to acidic dissolution, wipe-out of ZVIN, and demolished organic capping agents on ZVIN at low pH [38]. From the experimental data, it is observed that Cr (VI) removal efficiency of ZVIN decreases with the increase in pH of the solution. The reason may be explained at higher pH: (1) there is a competition between negatively charged hydroxyl ions and Cr(VI) which exists mainly in the form of oxyanions and (2) the oxide passivated film formed due to the decrease in iron corrosion production, which prevents further adsorption of Cr(VI) ions.

### 3.5.4 Effect of dosage of ZVIN on Cr(VI) removal

The amount of ZVIN varied (0.4, 0.8, 1.2, and 1.6 g/L) to determine the influence of dosage of ZVIN on Cr(VI) removal. In this study, it is noticed that the amount of ZVIN increases the rate of removal efficiency and is also increased due to the increase in the number of binding sites expected. However, Cr(VI) removal efficiency of ZVIN is not significantly less at the lower dosage but the adsorption process is much slower. At the higher dosage (1.6 g/L) of ZVIN, a rapid adsorption takes place and the equilibrium is attained within 10 min while at the lower dosage (0.4 g/L) the time required to attain equilibrium is 120 min.

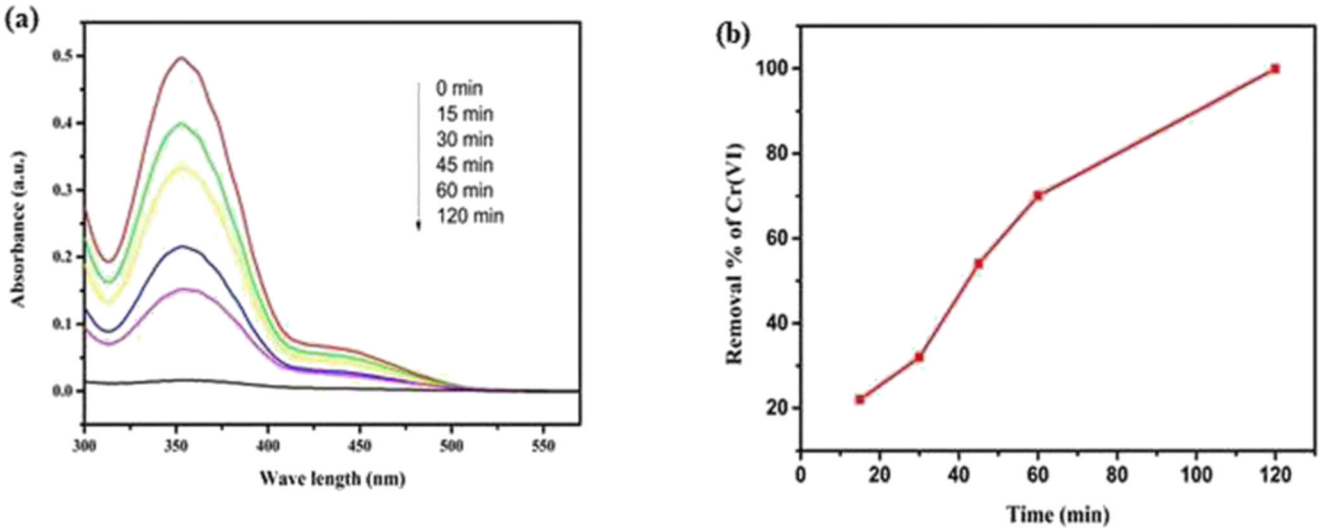


**Fig. 6** **a** The relative change in the concentration Cr(VI). (b) Effect of contact time on the % of removal of Cr (VI) using CR flower extract stabilized ZVIN

### 3.5.5 Adsorption isotherms

The linear plots of $1/q_e$ against $1/c_e$ show the Langmuir adsorption isotherm of Cr(VI) removal by CR flower extract stabilized ZVIN (Fig. 7a). The slope and intercept values of straight line give the parameters $X_m$ and $b$, respectively. The introductory information about substantive characteristics of Langmuir adsorption isotherm is provided by a dimensionless quantity $R_L$ (separation factor). If $0 < R_L < 1$, it is considered favorable adsorption; if $R_L > 1$, it is considered unfavorable adsorption; if $R_L = 0$, it is considered irreversible adsorption; if $R_L = 1$, it is considered linear adsorption [39]. The equation for $R_L$ is:

$$R_L = \frac{1}{1 + bc_0} \tag{7}$$

where $b$ (L/mg) is the Langmuir constant and $c_o$ (mg/L) is the initial concentration of adsorbate. In Table 1, the calculated Langmuir adsorption parameters are tabulated. $R_L$ value reveals the favorable adsorption of Cr(VI) on ZVIN. Based on the value of the correlation coefficient ($R^2$), it was clear that the Langmuir model was well fitted to experimental data.

Figure 7 shows the Freundlich adsorption isotherm of Cr(VI) removal by ZVIN. Freundlich constants $K_f$ and $n$ are determined using slope and intercept values of the straight line, respectively. However, from all these parameters, it was

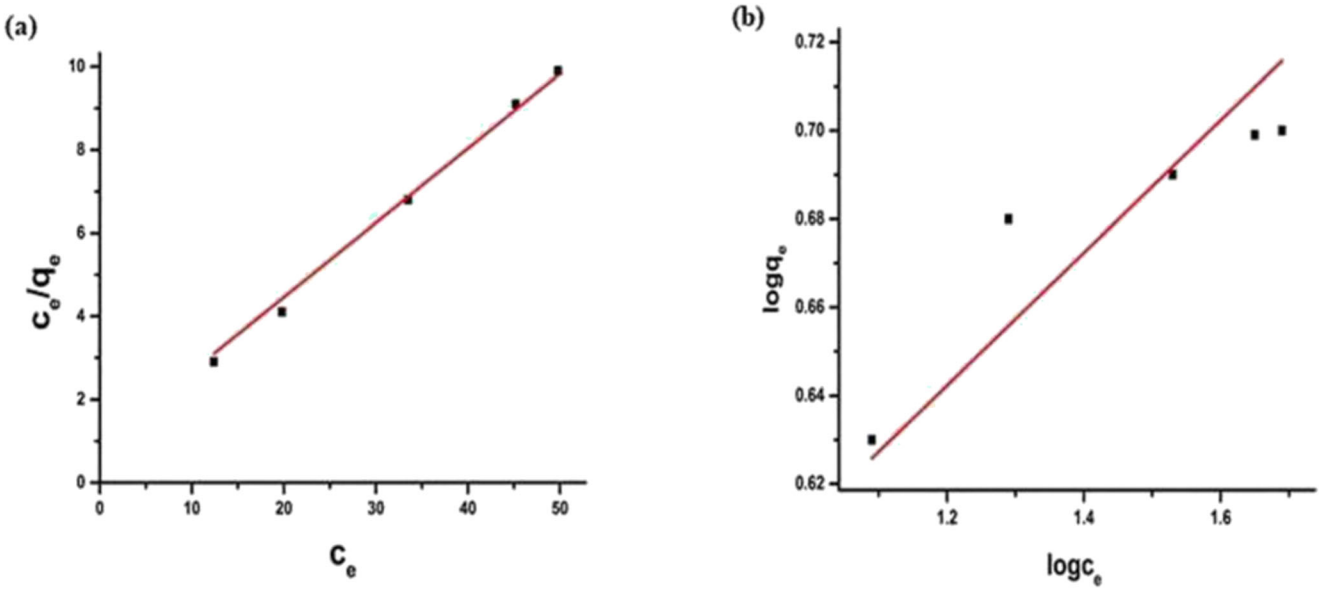


**Fig. 7** **a** Langmuir adsorption and **b** Freundlich adsorption isotherms of Cr(VI) removal using CR flower extract stabilized ZVIN

concluded that the Langmuir adsorption model was well fitted than the Freundlich adsorption model to the adsorption of Cr(VI) which confirms homogeneous and monolayer adsorption.

### 3.5.6 Adsorption kinetics

To examine the kinetics of Cr(VI) removal process by the synthesized CR flower extract stabilized ZVIN, the adsorption experiments were carried out at room temperature and the data well fitted to the pseudo-second-order kinetic model which can be expressed as:

$$q_t = \frac{k_2 t q_e^2}{1 + k_2 t q_e} \tag{8}$$

where $q_t$ (mg $g^{-1}$) is the amount of adsorbate adsorbed at time $t$ (min), $q_e$ (mg $g^{-1}$) is the equilibrium adsorption capacity of sorbent, and $k_2$ (g $mg^{-1}$ min) is the second-order rate constant. The linear form of pseudo-second-order kinetic model [40] is considered to determine the values of $k_2$ and $q_e$:

$$\frac{t}{q_t} = \frac{1}{k_2 q_e^2} + \frac{t}{q_e} \tag{9}$$

The values of $k_2$ and $q_e$ calculated from the slope and intercept values of the linear plot of $t/q_t$ against $t$ (Fig. 8) are summarized in Table 2.

## 4 Conclusions

In this summary, we report for the first time, the eco-friendly, non-toxic, and low-cost ZVIN synthesized by renewable and naturally occurring CR flower extract as both a reducing and stabilizing agent. The synthesized ZVIN were completely characterized by UV-vis, FT-IR, XRD, and SEM-EDX analysis for investigation of their optical, structural, and morphological properties. The UV-vis and FT-IR analyses confirm that the polyphenols and amino acids present in the flower extract are responsible for the formation of ZVIN. The crystallinity and size of the synthesized ZVIN are confirmed by XRD and SEM analysis. The estimated average size of ZVIN is less than 100 nm. The obtained results demonstrated that the synthesized ZVIN are very efficient in the adsorptive removal of Cr(VI) from contaminated water by Langmuir and Freundlich adsorption isotherms. The Langmuir isotherm was a well fit to the adsorption of Cr(VI) on ZVIN than the Freundlich isotherm and the adsorption process follows pseudo-second-order kinetics. The results of the graphs showed that the interaction effects of pH, ZVIN concentration, and contact time had the highest degree of influence on Cr(VI) removal efficiency, respectively. The optimum operation conditions were obtained with pH of aqueous solutions of 4.3, ZVIN concentration 1.6 g/L, and initial concentration of Cr(VI) is 10 ppm. In the future, this work was suggested for the removal of other pollutants from the wastewater in industrial applications.

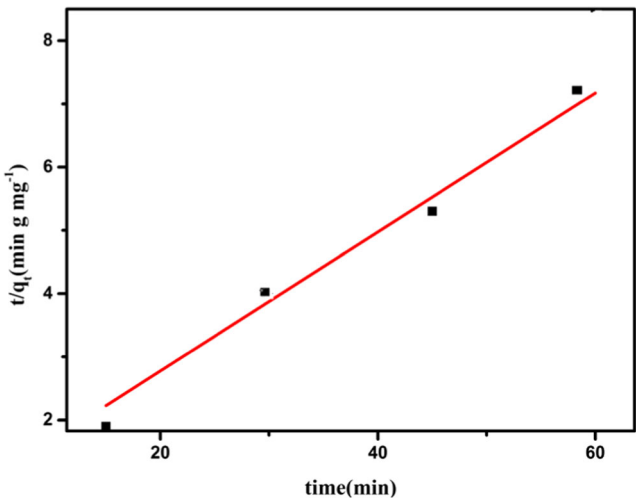


**Fig. 8** Pseudo-second-order kinetic plot of Cr(VI) removal using CR flower extract stabilized ZVIN

**Table 2** The calculated adsorption kinetic parameters for removal of Cr(VI) using ZVIN

| Initial conc. (mg $L^{-1}$) | $k_2$ (g $mg^{-1}$ min) | $q_e$ (mg $g^{-1}$) | $R^2$ |
|---|---|---|---|
| 10 | 0.027 | 9.09 | 0.99 |

**Acknowledgments** The authors are thankful to DST-FIST and Department of Chemistry, Osmania University, Hyderabad, India.

**Authors' contribution** All authors (KS, DA, PYS) have contributed to the writing of the manuscript. All authors read and approved the final manuscript.

## Compliance with ethical standards

**Competing interests** The authors declare that they have no competing interests.

## References

1. I. Ali, C. Peng, Z.M. Khan, I. Naz, M. Sultan, M. Ali, I.A. Abbasi, T. Islam, T. Ye, Overview of microbes based fabricated biogenic nanoparticles for water and wastewater treatment. J. Environ. Manag. **230**, 128–150 (2019)
2. X. Yin, W. Liu, J. Ni, Removal of coexisting Cr (VI) and 4-chlorophenol through reduction and Fenton reaction in a single system. Chem. Eng. J. **248**, 89–97 (2014)
3. J. Zhu, H. Gu, J. Guo, M. Chen, H. Wei, Z. Luo, N. Haldolaarachchige, Mesoporous magnetic carbon nanocomposite fabrics for highly efficient Cr (VI) removal. J. Mater. Chem. A **2**, 2256–2265 (2014)

4. N. Abdullah, N. Yusof, A.F. Ismail, F.E. Othman, J. Jaafar, L.W. Jye, W.N. Salleh, F. Aziz, N. Misdan, Effects of manganese (VI) oxide on polyacrylonitrile-based activated carbon nanofibers (ACNFs) and its preliminary study for adsorption of lead (II) ions. Emerg. Mater. **1**, 89–94 (2018)
5. D. Ayodhya, G. Veerabhadram, Preparation, characterization, photocatalytic, sensing and antimicrobial studies of Calotropis gigantea leaf extract capped CuS NPs by a green approach. J. Inorg. Organomet. Polym. Mater. **27**, 215–230 (2017)
6. X. Weng, X. Jin, J. Lin, R. Naidu, Z. Chen, Removal of mixed contaminants Cr (VI) and Cu (II) by green synthesized iron based nanoparticles. Ecol. Eng. **97**, 32–39 (2016)
7. R.M. Schneider, C.F. Cavalin, M.A.S.D. Barros, C.R.G. Tavares, Adsorption of chromium ions in activated carbon. Chem. Eng. J. **132**, 355–362 (2007)
8. K.C. Lai, I.M. Lo, Removal of chromium (VI) by acid-washed zero-valent iron under various groundwater geochemistry conditions. Environ. Sci. Technol. **42**, 1238–1244 (2008)
9. I. Ali, C. Peng, I. Naz, Z.M. Khan, M. Sultan, T. Islam, I.A. Abbasi, Phytogenic magnetic nanoparticles for wastewater treatment: a review. RSC Adv. **7**, 40158–40178 (2017)
10. I. Ali, C. Peng, Z.M. Khan, I. Naz, Yield cultivation of magnetotactic bacteria and magnetosomes: a review. J. Basic Microbiol. **57**, 643–652 (2017)
11. I. Ali, C. Peng, Z.M. Khan, I. Naz, M. Sultan, An overview of heavy metal removal from wastewater using magnetotactic bacteria. J. Chem. Technol. Biotechnol. **93**, 2817–2832 (2018)
12. I. Ali, Z.M. Khan, C. Peng, I. Naz, M. Sultan, M. Ali, M.H. Mahmood, Y. Niaz, Identification and elucidation of the designing and operational issues of trickling filter systems for wastewater treatment. Pol. J. Environ. Stud. **26**, 2431–2444 (2017)
13. V.K. Gupta, A. Rastogi, A.J. Nayak, Adsorption studies on the removal of hexavalent chromium from aqueous solution using a low cost fertilizer industry waste material. J. Colloid Interface Sci. **342**, 135–141 (2010)
14. E. Malkoc, Y. Nuhoglu, M. Dundar, Adsorption of chromium (VI) on pomace-an olive oil industry waste: batch and column studies. J. Hazard. Mater. **138**, 142–151 (2006)
15. H. Dang, Y. Zhang, P. Du, Enhanced removal of soluble Cr (VI) by using zero-valent iron composite supported by surfactant-modified zeolites. Water Sci. Technol. **70**, 1398–1404 (2014)
16. B. Calderon, A. Fullana, Heavy metal release due to aging effect during zero valent iron nanoparticles remediation. Water Res. **83**, 1–9 (2015)
17. Z. Zhou, D. Chaomeng, Z. Xuefei, Z. Jianfu, Z. Yalei, The removal of antimony by novel NZVI-zeolite: the role of iron transformation. Water Air Soil Pollut **226**, 76 (2015)
18. D. Ayodhya, G. Veerabhadram, Green synthesis, characterization, photocatalytic, fluorescence and antimicrobial activities of Cochlospermum gossypium capped $Ag_2S$ nanoparticles. J. Photochem. Photobiol. B **157**, 57–69 (2016)
19. D. Ayodhya, G. Veerabhadram, Sunlight-driven competent photocatalytic degradation of crystal violet using sonochemically produced GO capped $Ag_2S$ nanocomposites. Mat. Today Commun. **19**, 157–169 (2019)
20. M. Herlekar, S. Barve, R. Kumar, Plant-mediated green synthesis of iron nanoparticles. J. Nanopart. **2**, 9 (2014)
21. T. Wang, X. Jin, Z. Chen, M. Megharaj, R. Naidu, Green synthesis of Fe nanoparticles using eucalyptus leaf extracts for treatment of eutrophic wastewater. Sci. Total Environ. **466**, 210–213 (2014)
22. I. Ali, C. Peng, I. Naz, Removal of lead and cadmium ions by single and binary systems using phytogenic magnetic nanoparticles functionalized by 3-marcaptopropanic acid. Chin. J. Chem. Eng. **27**, 949–964 (2018)
23. K. Basavaiah, M.H. Kahsay, D. Ramadevi, Green synthesis of magnetite nanoparticles using aqueous pod extract of Dolichos lablab L for an efficient adsorption of crystal violet. Emerg. Mater. **1**, 121–132 (2018)
24. K. Sravanthi, D. Ayodhya, P.Y. Swamy, Green synthesis, characterization and catalytic activity of 4-nitrophenol reduction and formation of benzimidazoles using bentonite supported zero valent iron nanoparticles. Mater. Sci. Energy Technol. **2**, 298–307 (2019)
25. V. Madhavi, T.N.V.K.V. Prasasd, B.R.A. Vijaya, R.B. Ravindra, G. Madhavi, Application of phytogenic zero valent iron nanoparticles in the adsorption of hexavalent chromium. Spectrochim. Acta. A Mol. Biomol. Spectrosc. **116**(17–25), 17–25 (2013)
26. S.S. Poguberovic, D.M. Krcmar, S.P. Maletic, Z. Kónya, D.D.T. Pilipovic, D.V. Kerkez, S.D. Roncevic, Removal of As (III) and Cr (VI) from aqueous solutions using "green" zero-valent iron nanoparticles produced by oak, mulberry and cherry leaf extracts. Ecol. Eng. **90**, 42–49 (2016)
27. J. Eastoe, J.S. Dalton, Adv. Dynamic surface tension and adsorption mechanisms of surfactants at the air–water interface. J. Colloid Interface Sci **85**, 103–144 (2000)
28. K. Vijayaraghavan, T.V.N. Padmesh, K. Palanivelu, M. Velan, Biosorption of nickel (II) ions onto Sargassum wightii: application of two-parameter and three-parameter isotherm models. J. Hazard. Mater. **133**, 304–308 (2006)
29. K. Sravanthi, D. Ayodhya, P.Y. Swamy, Green synthesis, characterization of biomaterial-supported zero-valent iron nanoparticles for contaminated water treatment. J. Anal. Sci. Technol. **9**, 3 (2018)
30. A. Soliemanzadeh, M. Fekri, The application of green tea extract to prepare bentonite-supported nanoscale zero-valent iron and its performance on removal of Cr (VI): effect of relative parameters and soil experiments. Microporous Mesoporous Mater. **239**, 60–69 (2017)
31. R.K. Das, B.B. Borthakur, U. Bora, Green synthesis of gold nanoparticles using ethanolic leaf extract of Centella asiatica. Mater. Lett. **64**, 1445–1447 (2010)
32. T. Wang, J. Lin, Z. Chen, M. Megharaj, R. Naidu, Green synthesized iron nanoparticles by green tea and eucalyptus leaves extracts used for removal of nitrate in aqueous solution. J. Clean. Prod. **83**, 413–419 (2014)
33. A. Rao, A. Bankar, A.R. Kumar, S. Gosavi, S. Zinjarde, Removal of hexavalent chromium ions by Yarrowia lipolytica cells modified with phyto-inspired $Fe^0/Fe_3O_4$ nanoparticles. J. Contam. Hydrol. **146**, 63–73 (2013)
34. S. Machado, W. Stawinski, P. Slonina, A.R. Pinto, J.P. Grosso, H.P. Nouws, J.T. Albergaria, C. Delerue-Matosa, Application of green zero-valent iron nanoparticles to the remediation of soils contaminated with ibuprofen. Sci. Total Environ. **461**, 323–329 (2013)
35. T. Shahwan, S. AbuSirriah, M. Nairat, E. Boyac, A.E. Eroglu, T.B. Scott, K.R. Hallam, Green synthesis of iron nanoparticles and their application as a Fenton-like catalyst for the degradation of aqueous cationic and anionic dyes. Chem. Eng. J. **172**, 258–266 (2011)
36. S. Ghosh, W. Jiang, J.D. Mcclements, B. Xing, Colloidal stability of magnetic iron oxide nanoparticles: influence of natural organic matter and synthetic polyelectrolytes. Langmuir **27**, 8036–8043 (2011)
37. M. Gheju, I. Balcu, G. Mosoarca, Removal of Cr (VI) from aqueous solutions by adsorption on $MnO_2$. J. Hazard. Mater. **310**, 270–277 (2016)
38. Y. Zou, X. Wang, A. Khan, P. Wang, Y. Liu, A. Alsaedi, T. Hayat, X. Wang, Environmental remediation and application of nanoscale zero-valent iron and its composites for the removal of heavy metal ions: a review. Environ. Sci. Technol. **50**, 7290–7304 (2016)
39. H. Zheng, Y. Wang, Y. Zheng, H. Zhang, S. Liang, M. Long, Equilibrium, kinetic and thermodynamic studies on the sorption of 4-hydroxyphenol on Cr-bentonite. Chem. Eng. J. **143**, 117–123 (2008)
40. P.X. Wu, S.Z. Li, L.T. Ju, N.W. Zhu, J.H. Wu, P. Li, Z. Dang, Mechanism of the reduction of hexavalent chromium by organo-